

This is an accepted manuscript before typesetting. The final version of this manuscript will soon be published with the journal *Geology*. Please feel free to contact the authors, we welcome feedback

1 Simultaneous fall and flow during pyroclastic eruptions: a novel 2 proximal hybrid facies

3

4 **Natasha Dowey¹ and Rebecca Williams²**

5 *¹Department of the Natural and Built Environment, Sheffield Hallam University, UK, S1 1WB*

6 *²Department of Geography, Geology and Environment, University of Hull, UK, HU6 7RX*

7 **ABSTRACT**

8 The deposits of Plinian and sub-Plinian eruptions provide critical insights into past volcanic
9 events and inform numerical models that aim to mitigate against future hazards. However,
10 pyroclastic deposits are often considered from either a fallout or pyroclastic density current
11 (PDC) perspective, with little attention given to facies exhibiting characteristics of both
12 processes. Such hybrid units may be created where fallout and PDCs act simultaneously, where a
13 transitional phase between the two occurs, and/or due to reworking. This study presents analysis
14 of a novel hybrid pyroclastic lithofacies found on Tenerife and Pantelleria. The coarse pumice
15 block facies has an openwork texture and correlates with distal Plinian units, but is cross-
16 stratified and relatively poorly sorted with an erosional base. The facies is proposed to record the
17 simultaneous interaction of very proximal fallout with turbulent PDCs, and reveals a fuller
18 spectrum of hybrid deposition than previously reported. This work highlights the importance of
19 recognising hybrid deposition both in the rock record and hazard modelling.

20 **INTRODUCTION**

21 Analysis of pyroclastic stratigraphy can reveal the behaviour and magnitude of explosive
22 eruptions (e.g. Fisher and Schmincke, 1984), providing input parameters for numerical models

23 (e.g. Pyle, 1989; Bursik and Woods, 1996; Doyle et al., 2010) and informing hazard analysis
24 (e.g. Bonadonna et al., 2005). Pyroclastic deposits may be interpreted to record either plume
25 (fallout) or pyroclastic density current (lateral) activity. However, during an eruption multiple
26 processes related to the eruption column, fountaining and pyroclastic density currents (PDCs)
27 may impact the same location at the same time. Deposits that capture simultaneous processes are
28 common at tuff cones and maars (e.g. Cole et al., 2001; Zanon et al., 2009 and refs therein), but
29 there are relatively few studies of such hybrid deposits formed during Plinian eruptions (e.g.
30 Valentine and Giannetti, 1995). In this study, we (1) disentangle hybrid lithofacies using
31 previously reported examples, (2) define a new proximal hybrid lithofacies based on evidence
32 from the 273 ka Poris Formation of Tenerife and the 46 ka Green Tuff of Pantelleria, and (3)
33 discuss its significance for interpretation and modelling of volcanic hazards.

34 **HYBRID LITHOFACIES**

35 Deposits classified here as hybrid exhibit characteristics of both Plinian fallout (typically clast-
36 supported and landscape-mantling; e.g. Walker, 1971) and ignimbrite deposited by PDCs
37 (typically ash and pumice-rich and poorly sorted; e.g. Fisher and Schmincke, 1984). Hybrid
38 facies can vary in appearance; ignimbrite stratigraphy varies dependent on a range of factors
39 (such as PDC concentration, on a spectrum of fully dilute to fully concentrated) (e.g. Branney
40 and Kokelaar, 2002; Sulpizio et al., 2014), and Plinian fallout units are variable due to factors
41 including plume height and proximity to vent (e.g. Cioni et al., 2015).

42 **Simultaneous primary deposition**

43 Valentine & Giannetti (1995) describe a hybrid lithofacies generated by primary volcanic fallout
44 and PDC processes operating simultaneously within the White Trachytic Tuff, Roccamonfina,
45 Italy (subunit E₁). Associated ignimbrite is predominantly fine-grained ash, with minor pumice

46 lapilli. By contrast, the hybrid lithofacies is clast-supported and comprises angular pumices
47 ranging from coarse lapilli to small blocks. Pumice layers grade from ignimbrite, thicken and
48 thin, and pinch out laterally. The hybrid lithofacies is interpreted to record Plinian fallout into
49 dilute (ash-rich) PDCs that waxed and waned; the pumice fall was either incorporated into the
50 currents, or fell through them and dominated the deposition.

51 **Alternating primary deposition**

52 Alternating PDC and fallout units in volcanic successions may be interpreted as hybrid facies. A
53 spectrum of lithofacies architecture can occur at the base of ignimbrite successions, marking the
54 change from Plinian fallout to PDC deposition (see Valentine et al., 2019 for review). Modelling
55 has been used to propose that a ‘transitional regime’ can occur between the two end members
56 where the collapsing eruption column is oscillatory and highly unsteady (e.g. Neri and Dobran,
57 1994; Di Muro et al., 2004 and refs therein). Di Muro et al. (2008) describe a hybrid lithofacies
58 recording this transitional regime in the 800 BP Quilotoa succession, Ecuador. The A2 sub-
59 member of Unit U1 comprises alternating clast-supported pumice lapilli layers and beds of
60 stratified ash, pumice- and lithic-lapilli. Proximally, the facies is cross-stratified. Distally,
61 regressive and progressive bedforms occur and the facies grades laterally into a pumice lapilli
62 bed.

63 Alternating facies in the 1912 Novarupta proximal succession, Alaska, are interpreted by
64 Houghton et al. (2004) to reflect coeval regimes rather than plume oscillation. Unit Fall 2/PDC 2,
65 comprising up to seven PDC beds with thin intervening lapilli falls, is proposed to record fallout
66 deposited during intervals between discrete PDC units from a plume that maintained buoyant and
67 non-buoyant states simultaneously.

68 **Reworking and redeposition**

69 Deposits that exhibit characteristics of both fallout and PDC processes may be created by
70 reworking. Fallout units can be reworked by ambient wind or water during a hiatus in the
71 eruption (e.g. Yellowstone, Myers et al., 2016). The syn-eruptive involvement of strong wind
72 currents may create a lack of clear distinction between the deposits of Plinian fallout and a fully -
73 dilute PDC (Wilson and Houghton, 2000). Wilson & Hildreth (1998) describe a hybrid fall
74 deposit in the Bishop Tuff, California, distinguished by variable cross-bedding and the presence
75 of sub-rounded pumice lapilli, interpreted to record redeposition of Plinian fallout by wind
76 vortices driven by air currents into coeval PDCs.

77 **A NEW HYBRID LITHOFACIES**

78 Investigations of proximal pyroclastic stratigraphy are rare, in large part because of non-
79 preservation due to caldera collapse or erosion during eruption waxing. However, where
80 preserved, proximal exposures can give important insights into complex depositional processes
81 (e.g. Druitt and Sparks, 1982; Houghton et al., 2004). Here we report a proximal hybrid
82 lithofacies (referred to throughout as xspB) found at Las Cañadas Caldera, Tenerife and
83 Pantelleria, Italy.

84 **The Poris Formation, Tenerife**

85 Proximal deposits of the 273 ka Poris eruption are exposed at Las Cañadas less than 4 km from
86 the likely vent location, in the 1.9 km wide Diego Hernandez wall (Smith and Kokelaar, 2013).
87 Distal Poris exposures occur 15-20 km away in the coastal Bandas del Sur (e.g. Brown and
88 Branney, 2004).

89 The proximal Poris Formation includes a parallel-stratified to cross-stratified pumice-block
90 facies (xspB). Typically <2 m thick, xspB consists of pumice-rich beds 50-800 mm thick
91 bounded by ash-rich beds <100 mm thick (Smith and Kokelaar, 2013). Pumice beds are poorly

92 sorted (σ_{ϕ} 1.7, see Fig 1B for grainsize distribution), and typically contain 70-80% pumice lapilli
93 and blocks (5-300 mm) with rare lithic lapilli. At one location a pumice bed is fully clast-
94 supported (Fig. 2A). Pumices ≤ 20 mm in diameter are sub-rounded, while large lapilli and
95 blocks (20-300 mm) are sub-angular to angular. Pumice blocks show no evidence of ballistic
96 impact (such as sag structures or jigsaw-fit breakage). Pumice beds display planar and low-angle
97 cross-stratification (Fig 1A), and occasional internal cross-stratification of pumice clasts (Fig.
98 2B). Three dimensional cuts show that xspB beds thin and thicken both laterally and
99 longitudinally (Fig 1A). The xspB facies is in gradational to erosive contact with stratified lithic-
100 rich lapilli-tuff below, and is overlain by stratified to massive lapilli-tuff with a locally erosive
101 contact (Fig 1A). It is poorer in ash and lithic content (by 15% and 14% respectively at Fig. 1
102 locality) and better sorted than the massive lapilli-tuff. The xspB facies is distinct from bedded
103 pumice lapilli at the base of the succession by the pumice blocks (Fig, 2A), poorer sorting (σ_{ϕ}
104 1.7 versus σ_{ϕ} 1.3; Fig 1B), cross-stratification and variable ash content (Fig. 1A).
105 In distal Poris Formation exposures, two discrete clast-supported pumice lapilli facies record
106 Plinian fallout (members 1 and 5 of Brown and Branney, 2013). The proximal xspB facies
107 stratigraphically correlates with the upper distal fallout (Smith, 2012).

108 **The Green Tuff Formation, Pantelleria**

109 The 46 ka Green Tuff Formation is well exposed across Pantelleria, from the Cinque Denti
110 caldera walls (< 3 km from the vent) to coastal sections (< 7 km from the vent) (Williams, 2010;
111 Williams et al., 2014). In the Cinque Denti wall at Bagno dell'Acqua (Fig 3A), the proximal
112 Green Tuff Formation contains discontinuous horizons of a clast-supported, poorly-sorted (σ_{ϕ}
113 1.6, Fig 3B), cross-stratified pumice-block facies (xspB). The facies comprises angular pumice
114 lapilli and blocks (< 275 mm) and subordinate poly-lithic lapilli and blocks (< 77 mm) (Fig. 2C)

115 that are not systematically smaller than pumice clasts. Local lithic- and pumice-rich lenses (Fig
116 2D) occur within the unit. Cross-stratification in xspB is relatively high angle (~20-30°), not
117 unidirectional and transverse to inferred current direction. Locally, lithic-rich scours <300 mm
118 thick and <500 mm wide, >40% lithics, occur at the base of xspB, with basal contacts cutting
119 into the units below (Fig. 3A).

120 The xspB facies grades vertically from a massive pumice lapilli facies with a locally erosive
121 contact, and is overlain by welded ignimbrite; xspB is distinct from the underlying unit in that it
122 contains larger pumice and lithic blocks and exhibits poorer sorting (Fig. 3B), has a wider range
123 of lithic clast compositions, and is cross-stratified. It correlates compositionally (Zr ppm) and
124 stratigraphically with a pumice (or ash) fall layer in coastal sections (Williams et al., 2014).

125 **Interpretation**

126 The xspB facies differs from proximal lithic-rich breccias (e.g. Druitt and Sparks, 1982). It is
127 dominated by pumice (with exception of minor lithic-rich lenses at Pantelleria), does not contain
128 grading or elutriation pipes, and does not grade laterally into ignimbrite. The xspB facies has
129 similarities to fines-poor ignimbrite (e.g. Walker et al., 1980); it is better sorted and coarser than
130 massive lapilli-tuff, and less well sorted than associated Plinian deposits. However, xspB is not
131 massive, does not occur just locally (at Tenerife it is continuous across the caldera wall) and
132 correlates laterally with Plinian fallout. The cross-stratification makes xspB distinct from
133 reported proximal fallout, such as the coarse, poorly sorted 'Bed S' of the 1912 Novarupta
134 eruption that records complex fallout from a 'collar' of low-fountaining ejecta (Fierstein et al.,
135 1997). However, like Bed S, xspB contains distinctly coarse and poorly sorted pumice blocks.
136 The xspB facies exhibits characteristics of both fallout and PDC deposits. The sub-angular
137 pumice blocks, areal continuity, (variable) openwork texture, and correlation with Plinian units

138 are suggestive of fallout (e.g. Walker, 1971). The cross-stratification, relatively poor sorting,
139 erosional base, and lack of aerodynamic equivalence between adjacent clasts suggest PDC
140 deposition (e.g. Branney and Kokelaar, 2002). The xspB facies differs from previously reported
141 hybrid facies. It has a different grainsize to associated Plinian fallout (Figs 1B and 3B), and at
142 Pantelleria displays higher-angle cross-stratification than the hybrid facies created by fallout into
143 dilute PDCs described by Valentine and Gianetti (1995). It does not always directly overlie
144 Plinian fallout facies (Tenerife), nor does it contain interbedded strata (cf. Di Muro et al., 2008).
145 However, the dominance of pumice blocks is akin to the coarse proximal fallout layers in the
146 alternating Fall 2/PDC 2 sequence at Novarupta (Houghton et al., 2004). The xspB facies is
147 interpreted to record primary volcanic deposition; the proximal location makes extensive
148 aqueous reworking unlikely as there is no catchment or upslope source. The componentry of
149 xspB differs to underlying and coeval pumice fall deposits making clear-air reworking of those
150 facies unlikely (cf. Wilson and Hildreth, 1998).

151 At Tenerife and Pantelleria, the increase in grainsize in xspB relative to underlying facies records
152 an influx of coarser material at the vent. This may be due to vent widening and shallower
153 fragmentation (evidenced by coarse lithics within the lithofacies at Pantelleria and underlying
154 lithic-rich stratified tuff at Tenerife; Smith and Kokelaar, 2013). As coarse material entered the
155 column, large blocks were deposited from a low-fountaining collar of fallout ejecta (as invoked
156 by Fierstein et al., 1997) and smaller material was transported in PDCs formed by
157 contemporaneous fountaining.

158 In the Poris eruption, PDC activity had begun prior to deposition of xspB (recorded in underlying
159 tuff deposits: Brown and Branney, 2004; Smith and Kokelaar, 2013), but was unsteady and
160 marked by waxing and waning that led to changes in runout distance. During deposition of the

161 xspB facies (~4 km from likely vent), a hiatus in distal PDC activity allowed contemporaneous
162 Plinian fallout to be recorded at the coast (Dowey et al., 2020). On Pantelleria, xspB marks the
163 onset of PDC activity, indicating that the vent widening episode may have instigated column
164 collapse. The proximal currents did not travel far (<1 km); xspB is not longitudinally extensive
165 and is absent at distal locations.

166 The xspB facies reported here contains predominantly coarse material with variable fines, and
167 exhibits cross-stratification. Cross-stratification indicates traction-dominated deposition and
168 migration of bedforms at the flow boundary zone (sensu Branney and Kokelaar, 2002). This has
169 typically been associated with fully-dilute PDCs (aka surges), but is also possible in dense
170 granular currents (e.g. Smith et al., 2020). The range of grainsize evident in xspB, and evidence
171 of abrasion of the smaller pumices, indicates that the currents involved were not fully-dilute or
172 ash-rich (cf. Valentine and Giannetti, 1995). Minor fines-rich zones may have been generated by
173 changes in supply to the flow-boundary zone, or variable influence of fallout material.

174 We propose that the hybrid xspB facies reported here formed during a short-lived phase where
175 very proximal fallout interacted with turbulent density currents, in a setting similar to the
176 “impact zone” envisaged by Valentine (2020).

177 **SIGNIFICANCE**

178 This study provides a novel example of simultaneous primary volcanic deposition in the complex
179 proximal domain, representing a previously unreported part of the spectrum of hybrid deposition.
180 Numerical modelling exploring proximal ignimbrite-forming processes has shown that an influx
181 of coarse material into a collapsing column can translate into formation of dense flows in a
182 proximal “impact zone”, which are overridden by dilute currents of expelled fines (Valentine,
183 2020 and refs therein). This modelling could explain the fines-poor nature of the xspB facies

184 reported here. Greater recognition of hybrid processes in the rock record can inform future
185 modelling, allowing us to more confidently understand how fallout and flow may interact and
186 impact hazard assessments around a volcano.

187 It is important to recognise the “grey areas” in field volcanology. It is widely appreciated that
188 complexities such as bypass and erosion are inherent aspects of PDC activity that can be cryptic
189 in the rock record (e.g. Brown and Branney, 2004). Hybrid processes may be similarly cryptic.
190 Hybrid facies created by reworking during hiatuses can only be preserved where not eroded by a
191 subsequent PDC. Those recording Plinian fallout into a PDC are likely only recorded where
192 currents wane sufficiently to allow fallout to dominate the deposit or where Plinian material is
193 coarse/dominant enough to be recognised (this study).

194 We suggest that hybrid processes should be seen as inherent in Plinian eruptions and given
195 greater consideration. Different hybrid processes are likely to occur both at different locations
196 around the volcano, and at different stages of an eruption. A snapshot of this complexity is
197 illustrated in Fig. 4. It follows that hybrid pyroclastic units may be more common than is
198 reported. Where recorded, they can be difficult to distinguish from fallout or PDC deposits. An
199 interpretation of ignimbrite may lead to the involvement of fallout being underestimated, whilst
200 identification as fallout could lead to the existence of PDCs at a study location being overlooked.
201 Whatever the location on the volcano, correct hazard identification is the ideal; but perhaps just
202 as important to hazard modelling and assessment is acknowledgement of the potential
203 complexity and uncertainty highlighted by studies such as this.

204 **ACKNOWLEDGMENTS**

205 We acknowledge NERC studentships NE/G523855/1 and NER/S/A/2006/14156. We thank P.
206 Rowley, D. Brown, G. Valentine and C. Wilson for their reviews.

207 **REFERENCES CITED**

- 208 Bonadonna, C., Connor, C.B., Houghton, B.F., Connor, L., Byrne, M., Laing, A., and Hincks,
209 T.K., 2005, Probabilistic modeling of tephra dispersal: Hazard assessment of a multiphase
210 rhyolitic eruption at Tarawera, New Zealand: *Journal of Geophysical Research*, v. 110,
211 B03203, doi:10.1029/2003JB002896.
- 212 Branney, M.J., and Kokelaar, P., 2002, *Pyroclastic Density Currents and the Sedimentation of*
213 *Ignimbrites*: Geological Society of London Memoir no. 27 143pp
214 doi:10.1144/gsl.mem.2003.027.
- 215 Brown, R.J., and Branney, M.J., 2004, Event-stratigraphy of a caldera-forming ignimbrite
216 eruption on Tenerife: The 273 ka Poris Formation: *Bulletin of Volcanology*, v. 66, p. 392–
217 416, doi:10.1007/s00445-003-0321-y.
- 218 Brown, R.J., and Branney, M.J., 2013, Internal flow variations and diachronous sedimentation
219 within extensive, sustained, density-stratified pyroclastic density currents flowing down
220 gentle slopes, as revealed by the internal architectures of ignimbrites on Tenerife: *Bulletin*
221 *of Volcanology*, v. 75(7) doi:10.1007/s00445-013-0727-0.
- 222 Bursik, M.I., and Woods, A.W., 1996, The dynamics and thermodynamics of large ash flows:
223 *Bulletin of Volcanology*, v. 58, p. 175–193. doi: 10.1007/s004450050134
- 224 Cioni, R., Pistolesi, M., and Rosi, M., 2015, Plinian and Subplinian Eruptions, *in* Sigurdsson, H.
225 ed., *Encyclopedia of Volcanoes* (2nd Edition), Academic Press, p. 519–535, doi:
226 <https://doi.org/10.1016/C2015-0-00175-7>.
- 227 Cole, P.D., Guest, J.E., Duncan, A.M., and Pacheco, J.M., 2001, Capelinhos 1957-1958, Faial,
228 Azores: Deposits formed by an emergent Surtseyan eruption: *Bulletin of Volcanology*, v.
229 63, p. 204–220, doi:10.1007/s004450100136.

230 Di Muro, A., Neri, A., and Rosi, M., 2004, Contemporaneous convective and collapsing eruptive
231 dynamics: The transitional regime of explosive eruptions: *Geophysical Research Letters*, v.
232 31, L10607 doi:10.1029/2004GL019709.

233 Di Muro, A., Rosi, M., Aguilera, E., Barbieri, R., Massa, G., Mundula, F., and Pieri, F., 2008,
234 Transport and sedimentation dynamics of transitional explosive eruption columns: The
235 example of the 800 BP Quilotoa plinian eruption (Ecuador): *Journal of Volcanology and*
236 *Geothermal Research*, v. 174, p. 307–324, doi:10.1016/j.jvolgeores.2008.03.002.

237 Dowey, N.J., Kokelaar, B.P., and Brown, R.J., 2020, Counting currents: correlating flow units to
238 understand how pyroclastic density currents wax and wane in time and space. *Volcanic and*
239 *Magmatic Studies Group Annual Conference*, Plymouth. [https://vmmsg.org.uk/wp-](https://vmmsg.org.uk/wp-content/uploads/2020/01/Abstract_Volume_Plym2020.pdf)
240 [content/uploads/2020/01/Abstract_Volume_Plym2020.pdf](https://vmmsg.org.uk/wp-content/uploads/2020/01/Abstract_Volume_Plym2020.pdf)

241 Doyle, E.E., Hogg, A.J., Mader, H.M., and Sparks, R.S.J., 2010, A two-layer model for the
242 evolution and propagation of dense and dilute regions of pyroclastic currents: *Journal of*
243 *Volcanology and Geothermal Research*, v. 190, p. 365–378,
244 doi:10.1016/j.jvolgeores.2009.12.004.

245 Druitt, T.H., and Sparks, R.S.J., 1982, A proximal ignimbrite breccia facies on Santorini, Greece:
246 *Journal of Volcanology and Geothermal Research*, v. 13, p. 147–171, doi:10.1016/0377-
247 0273(82)90025-7.

248 Fierstein, J., Houghton, B.F., Wilson, C.J.N., and Hildreth, W., 1997, Complexities of plinian
249 fall deposition at vent: An example from the 1912 Novarupta eruption (Alaska): *Journal of*
250 *Volcanology and Geothermal Research*, v. 76, p. 215–227, doi:10.1016/S0377-
251 0273(96)00081-9.

252 Fisher, R. V., and Schmincke, H.-U., 1984, *Pyroclastic Flow Deposits*, in *Pyroclastic Rocks*,

253 Springer, Berlin, Heidelberg, p. 186–230, doi:10.1007/978-3-642-74864-6_8.

254 Houghton, B.F., Wilson, C.J.N., Fierstein, J., and Hildreth, W., 2004, Complex proximal
255 deposition during the Plinian eruptions of 1912 at Novarupta, Alaska: *Bulletin of*
256 *Volcanology*, v. 66, p. 95–133, doi:10.1007/s00445-003-0297-7.

257 Myers, M.L., Wallace, P.J., Wilson, C.J.N., Morter, B.K., and Swallow, E.J., 2016, Prolonged
258 ascent and episodic venting of discrete magma batches at the onset of the Huckleberry
259 Ridge supereruption, Yellowstone: *Earth and Planetary Science Letters*, v. 451, p. 285–297,
260 doi:10.1016/j.epsl.2016.07.023.

261 Neri, A., and Dobran, F., 1994, Influence of eruption parameters on the thermofluid dynamics of
262 collapsing volcanic columns: *Journal of Geophysical Research: Solid Earth*, v. 99, p.
263 11833–11857, doi:10.1029/94JB00471.

264 Pyle, D.M., 1989, The thickness, volume and grainsize of tephra fall deposits: *Bulletin of*
265 *Volcanology*, v. 51, p. 1–15.

266 Smith, N., 2012, Near-vent processes of the 273 ka Poris eruption (Tenerife): PhD thesis,
267 University of Liverpool, 300 p., <https://livrepository.liverpool.ac.uk/6253/>.

268 Smith, N.J., and Kokelaar, B.P., 2013, Proximal record of the 273 ka Poris caldera-forming
269 eruption, Las Cañadas, Tenerife: *Bulletin of Volcanology*, v. 75, 768, doi:10.1007/s00445-
270 013-0768-4.

271 Smith, G., Rowley, P., Williams, R., Giordano, G., Trolese, M., Silleni, A., Parsons, D.R., and
272 Capon, S., 2020, A bedform phase diagram for dense granular currents: *Nature*
273 *Communications*, v. 11, 2873 doi:10.1038/s41467-020-16657-z.

274 Sulpizio, R., Dellino, P., Doronzo, D.M., and Sarocchi, D., 2014, Pyroclastic density currents:
275 state of the art and perspectives: *Journal of Volcanology and Geothermal Research*, v. 283,

276 p. 36–65, doi: 10.1016/j.jvolgeores.2014.06.014

277 Valentine, G.A., 2020, Initiation of dilute and concentrated pyroclastic currents from collapsing
278 mixtures and origin of their proximal deposits: *Bulletin of Volcanology* 2020 82, 20
279 doi:10.1007/S00445-020-1366-X.

280 Valentine, G.A., and Giannetti, B., 1995, Single pyroclastic beds deposited by simultaneous
281 fallout and surge processes: Roccamonfina volcano, Italy: *Journal of Volcanology and*
282 *Geothermal Research*, v. 64, p. 129–137, doi:10.1016/0377-0273(94)00049-M.

283 Valentine, G.A., Palladino, D.M., DiemKaye, K., and Fletcher, C., 2019, Lithic-rich and lithic-
284 poor ignimbrites and their basal deposits: Sovana and Sorano formations (Latera caldera,
285 Italy): *Bulletin of Volcanology* 2019 81, 29 doi:10.1007/S00445-019-1288-7.

286 Walker, G.P.L., 1971, Grain-size characteristics of pyroclastic deposits: *The Journal of Geology*,
287 79 (6) p. 696–714, doi:10.1086/627699.

288 Walker, G.P.L., Wilson, C.J.N., and Frogatt, P.C., 1980, Fines-depleted ignimbrite in New
289 Zealand — The product of a turbulent pyroclastic flow: *Geology*, v. 8 (5), p. 245–249. Doi:
290 [https://doi.org/10.1130/0091-7613\(1980\)8%3C245:FIINZT%3E2.0.CO;2](https://doi.org/10.1130/0091-7613(1980)8%3C245:FIINZT%3E2.0.CO;2)

291 Williams, R., 2010, Emplacement of radial pyroclastic density currents over irregular
292 topography: the chemically-zoned, low aspect-ratio Green Tuff ignimbrite, Pantelleria,
293 Italy: PhD thesis, University of Leicester.

294 Williams, R., Branney, M.J., and Barry, T.L., 2014, Temporal and spatial evolution of a waxing
295 then waning catastrophic density current revealed by chemical mapping: *Geology*, v. 42, p.
296 107–110, doi:10.1130/G34830.1.

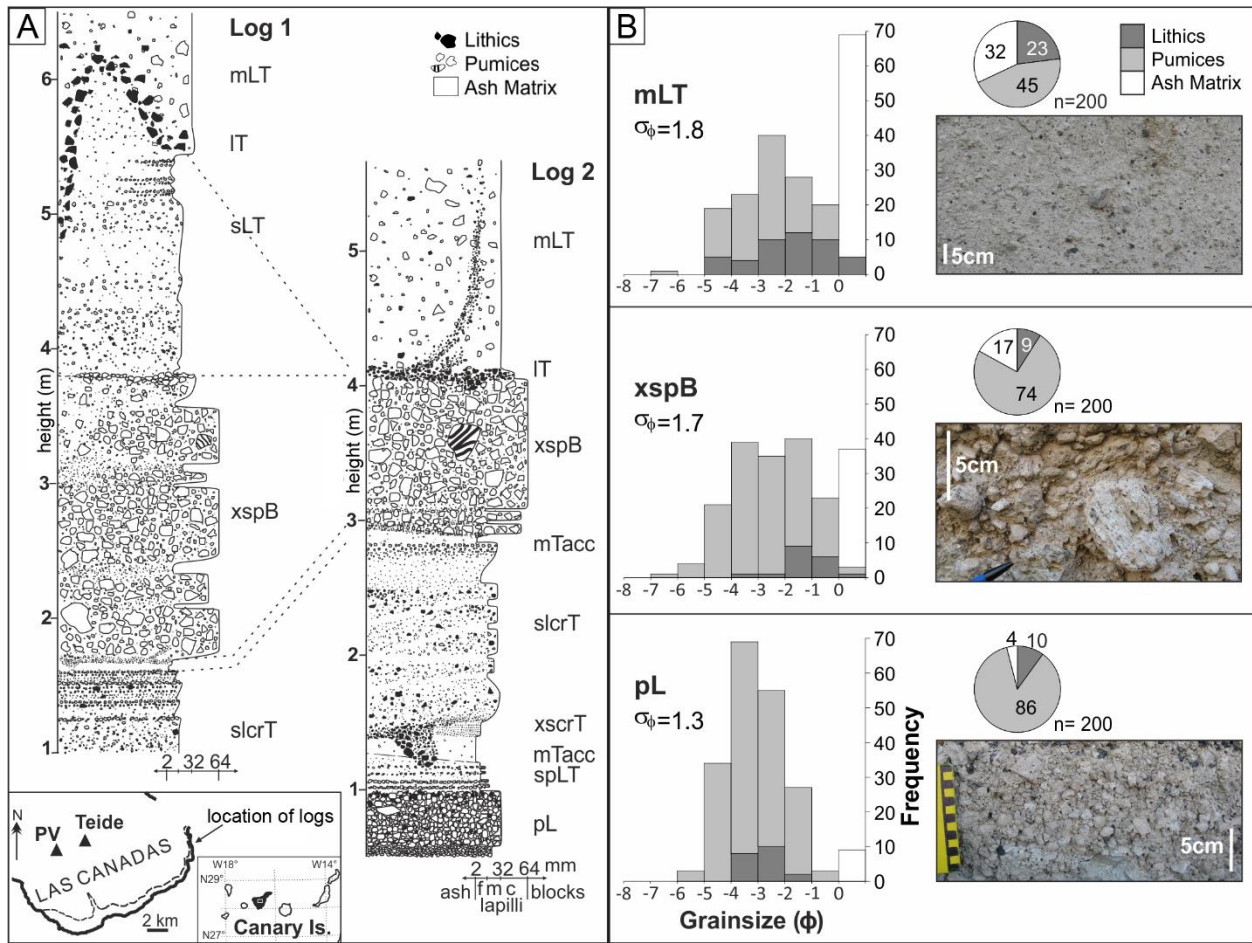
297 Wilson, C.J.N., and Hildreth, W., 1998, Hybrid fall deposits in the Bishop Tuff, California: A
298 novel pyroclastic depositional mechanism: *Geology*, v. 26, p. 7–10. doi:

299 [https://doi.org/10.1130/0091-7613\(1998\)026%3C0007:HFDITB%3E2.3.CO;2](https://doi.org/10.1130/0091-7613(1998)026%3C0007:HFDITB%3E2.3.CO;2)
300 Wilson, C.J.N., and Houghton, B.F., 2000, Pyroclast transport and deposition, *in* Sigurdsson, H.,
301 Houghton, B.F., Rymer, H., Stix, J., and McNutt, S. eds., *Encyclopedia of Volcanoes*, San
302 Diego, Academic Press, p. 545–554.
303 Zanon, V., Pacheco, J., and Pimentel, A., 2009, Growth and evolution of an emergent tuff cone:
304 Considerations from structural geology, geomorphology and facies analysis of São Roque
305 volcano, São Miguel (Azores): *Journal of Volcanology and Geothermal Research*, v. 180, p.
306 277–291, doi:10.1016/j.jvolgeores.2008.09.018.

307

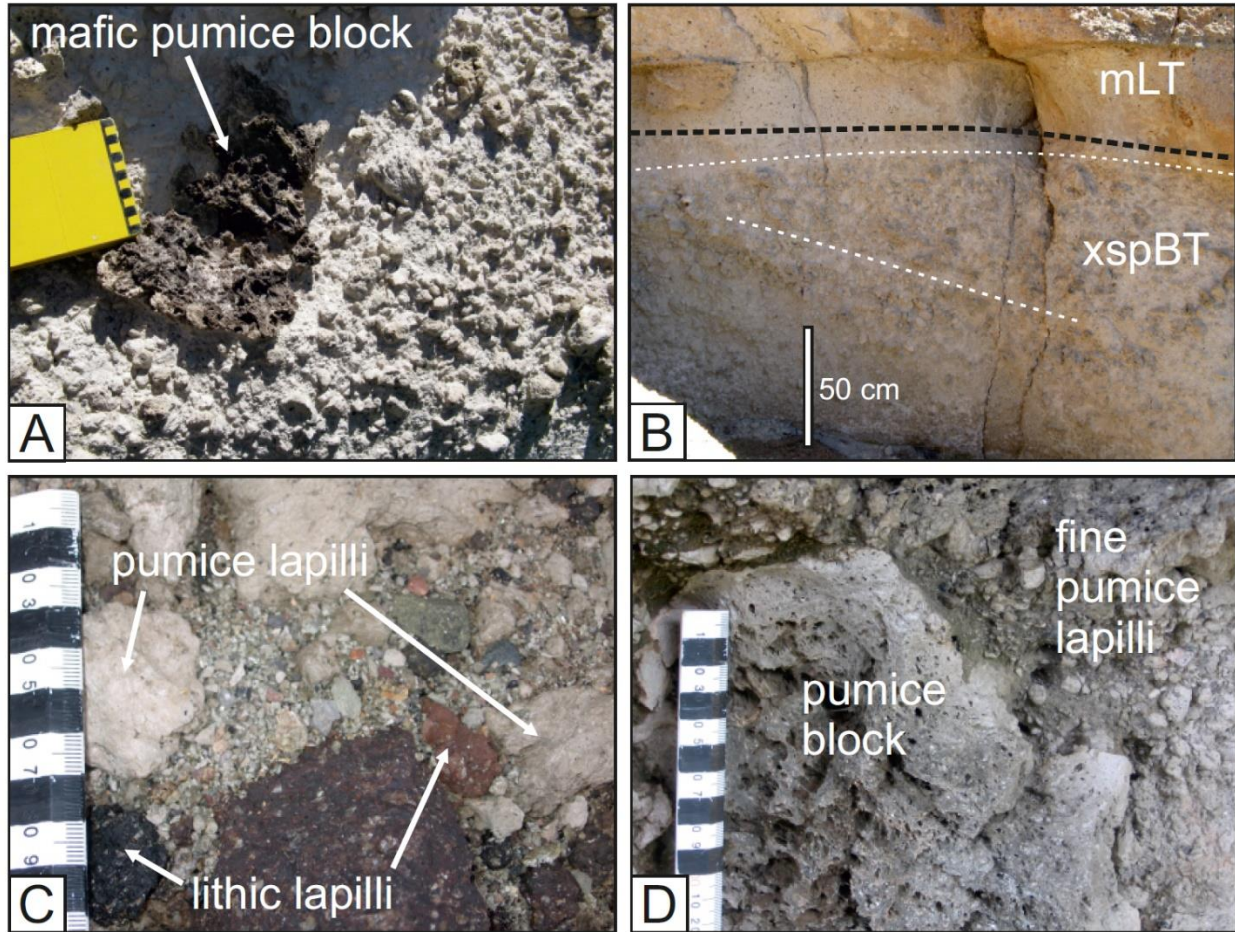
308 **SUPPLEMENTARY DATA**

309 Methods and imagery

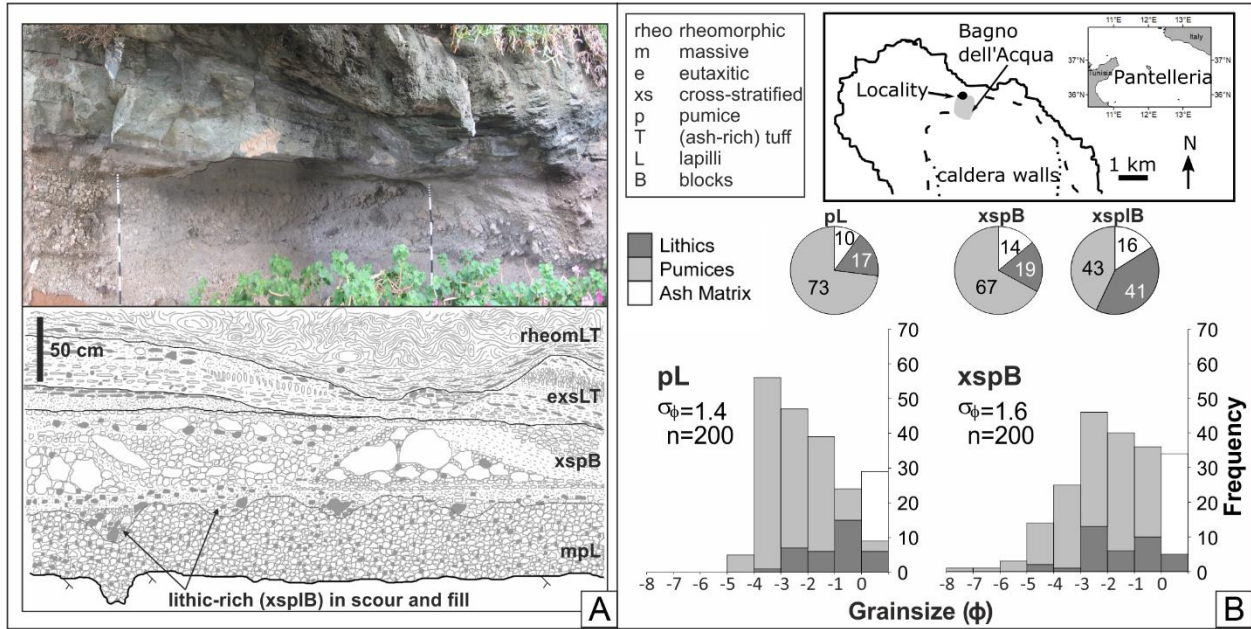


310

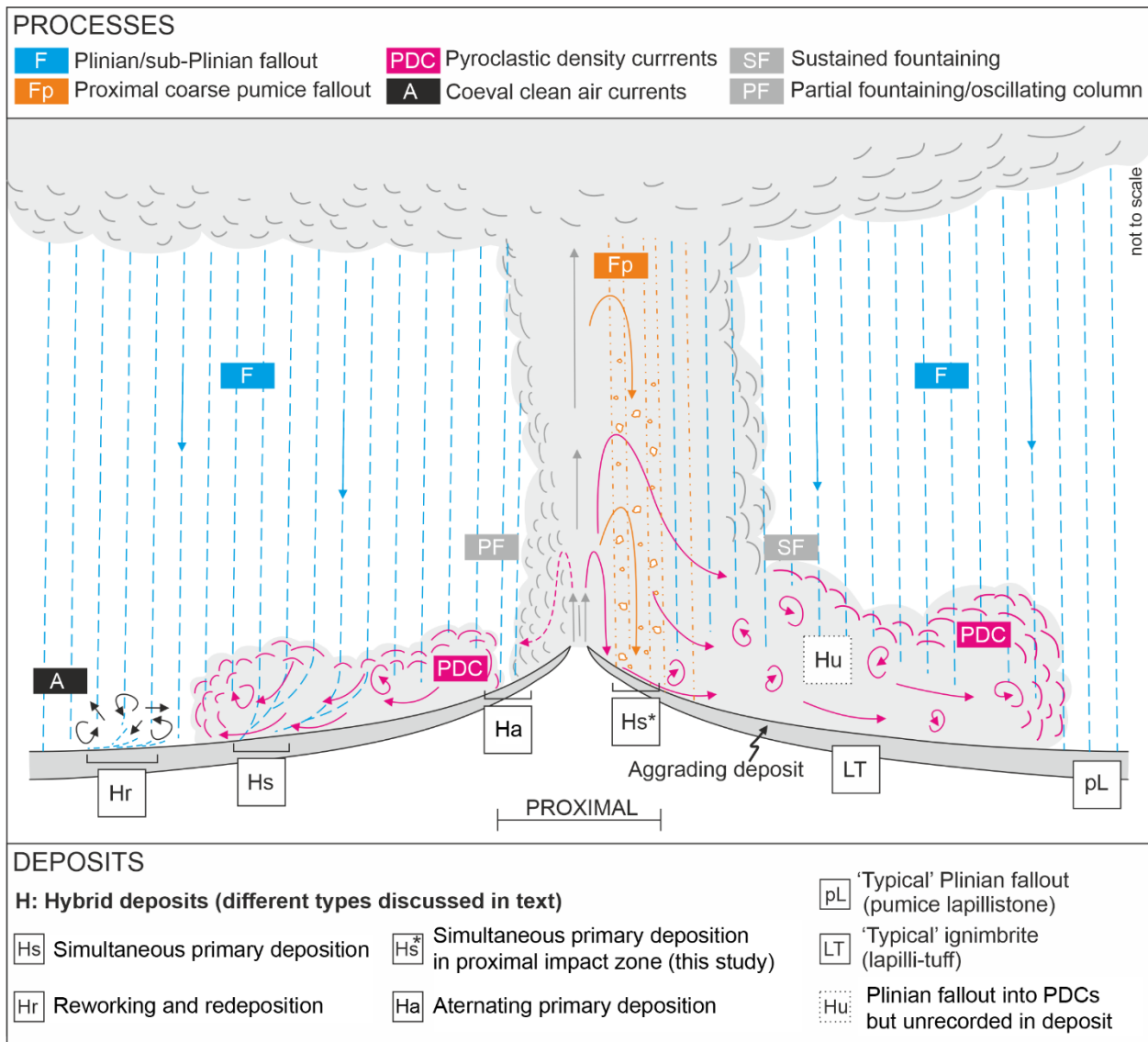
311 **Figure 1: (A) The xspB facies at Las Cañadas (inset; stratigraphic logs 20 m apart at**
 312 **28.280273, -16.549526). Facies abbreviation key shown in Figure 3. (B) Grainsize**
 313 **distribution histograms and pie charts illustrate comparative grainsize, sorting and**
 314 **componentry (see Supplement).**



315
 316 **Figure 2: The xspB facies at Las Cañadas [(A) clast supported, with phonotephrite pumice**
 317 **block (28.270853, -16.545632); (B) exhibiting internal cross stratification (28.267141, -**
 318 **16.546145)] and at Bagno dell'Acqua (36.819358, 11.988439) [(C) poorly-sorted poly lithic-**
 319 **rich lens; (D) coarse pumice blocks alongside more rounded pumice lapilli (scale in 10**
 320 **mm)].**



321
 322 **Figure 3: (A) Photo panel depicting xspB at Bagno dell'Acqua (inset; 36.819358,**
 323 **11.988439), atop pumice lapillistone and overlain by eutaxitic, cross-stratified lapilli-tuff.**
 324 **(B) Grainsize distribution histograms and pie charts illustrate comparative grainsize,**
 325 **sorting and componentry (see Supplement).**



326

327 **Figure 4: Schematic of a Plinian eruption summarising styles of hybrid deposition**

328 **discussed in the text. Coloured boxes define processes and white boxes are deposit types.**